

A Constitutive Model With Damage for  
High Temperature Superalloys\*

J.A. Sherwood and D.C. Stouffer  
Department of Aerospace Engineering  
and Engineering Mechanics  
University of Cincinnati  
Cincinnati, Ohio 45221

I. Introduction

The goal of the research is to develop a unified constitutive model that is applicable for high temperature superalloys used in modern gas turbines. The formulation will be considered successful if: (1) the resulting formulation is efficient for numerically intensive computation such as found in nonlinear finite element models, (2) there is a direct correspondence between the material parameters and experimental data, and (3) the resulting formulations are reasonably accurate for a variety of loading conditions.

Two unified inelastic state variable constitutive models have been evaluated for use with the damage parameter proposed by Kachanov [1]. The first is the model of Bodner and Partom [2,3] in which hardening is modeled through the use of a single state variable that is similar to drag stress. The other constitutive model is an extension of the Bodner-Partom flow proposed by Ramaswamy [4] that employs both a drag stress and back stress. This extension has been successful for predicting the tensile, creep, fatigue, torsional and nonproportional response of Rene' 80 at several

---

\* This research was supported, in part, by the National Aeronautics and Space Administration Lewis Research Center and the Air Force Wright Aeronautical Laboratory at Wright Patterson Air Force Base by grant NAG-3-511 to the University of Cincinnati.

temperatures. In both formulations a cumulative damage parameter is introduced to model the changes in material properties due to the formation of microcracks and microvoids that ultimately produce a macroscopic crack. Calculations have shown that the drag stress/damage model is reasonable for predicting the tensile and creep responses of IN100 at 1350°F and Rene' 95 at 1200°F, but the model is not entirely satisfactory for predicting the cyclic response of these materials. In this study a back stress/drag stress/damage model has been evaluated for Rene' 95 at 1200°F and is shown to predict the tensile, creep, and cyclic loading responses reasonably well.

## II. Drag Stress/Damage Model

The initial phase of this research is based on a constitutive model using only one hardening variable,  $Z$ , to simulate the drag stress of the material and a damage variable,  $\omega$ , to model the changes in the material properties due the formation of microcracks and microvoids. The inelastic flow equation of Bodner was used in the following form

$$\dot{\epsilon}_{ij}^I = D_0 \exp\left(-\frac{n+1}{2n}\left(\frac{Z^2(1-\omega)^2}{J_2}\right)^n\right) \frac{S_{ij}}{\sqrt{J_2}}, \quad (1)$$

where  $S_{ij}$  is the deviatoric stress tensor and  $J_2 = S_{ij} S_{ij}$ . The value of  $n$  controls strain rate sensitivity and  $D_0$  is the limiting strain rate. The evolution equations for the state variables  $Z$  and  $\omega$  were developed using the Hemholtz free energy as potential function similar to the work in [7]. The results show that the flow law and evolution equations are thermodynamically associated and are not free to be derived independently.

The damage parameter, as proposed by Kachanov, was defined to exist on the interval  $[0,1]$ . A value of zero represents no damage and a value of one for  $\omega$  denotes complete failure. Calculations for Rene' 95 and IN100

indicated that a value for the damage state variable of much less than one corresponds to failure.

The values of the material constants and initial value of the state variables were determined from experimental data that was obtained in a previous study. The experimental work was conducted by the Air Force Wright Aeronautical Laboratory, WPAFB, Ohio and Mars-Test Inc., Cincinnati, Ohio [5,6]. The correlation of the constitutive model to experimental observations of monotonic tensile and creep tests on IN100 at 1350°F and Rene' 95 at 1200°F was very good. The calculated response for IN100 is shown in Figures 1 and 2.

Extending the drag stress/damage model to predict fatigue loop responses was not completely successful. The model appeared to have trouble capturing the shape of the fatigue loop. This shortcoming is possibly due to how the state variable  $Z$  quantifies dislocation movements for a particular type of loading. Drag stress is metallurgically associated with the retardation of dislocation movement due to the interaction with precipitates which results in dislocation jogs or looping for example. Back stress is associated with the pile-up of dislocations at a barrier, such as a grain boundary, which cannot be overcome. During cyclic loading the back stress oscillates with the applied load while the drag stress either increases monotonically or remains essentially constant. Since the dislocation movement was only in one direction for the tensile and creep tests, the contributions of the drag stress and back stress to the total resistance of dislocation motion could be simulated by one state variable monotonically increasing to a steady state value. Although this lumping of resistances to dislocation motion worked well for monotonic loadings, it appears inadequate for cyclic loadings.

### III. Drag Stress/Back Stress/Damage Model

Based on the metallurgical considerations given above and the success of the drag stress/back stress model proposed by Ramaswamy for predicting the fatigue response of Rene' 80, a drag stress/back stress/damage model is proposed. The drag stress scalar  $Z$  simulates long term cyclic hardening while the back stress tensor  $\Omega_{ij}$  models the short term strain or work hardening. The governing equations are:

Inelastic Flow Equation,

$$\dot{\epsilon}_{ij}^I = D_0 \exp - \left[ \left( \frac{Z^2(1-\omega)^2}{3K_2} \right)^n \right] \frac{(S_{ij} - \Omega_{ij})}{\sqrt{K_2}} \quad (2)$$

Back Stress Evolution Equation,

$$\dot{\Omega}_{ij} = f_1 \dot{\epsilon}_{ij}^I + f_1 |\dot{\epsilon}_{ij}^I| \Omega_{ij} / \Omega_s + f_3 \dot{\sigma}_{ij} \quad (3)$$

Drag Stress Evolution Equation,

$$\dot{Z} = m(Z_1 - Z) \dot{W}^I \quad (4)$$

Damage Evolution Equation,

$$\dot{\omega} = g_2 \dot{\epsilon}_{\max}^{IT} \quad (5)$$

and

Back Stress Relaxation Equation

$$\dot{\Omega}_s = -B \left( \frac{\sqrt{J_2}}{\sigma_0} \right)^r (\Omega_s - \Omega_{\text{sat}}) \quad (6)$$

where  $K_2 = (S_{ij} - \Omega_{ij})(S_{ij} - \Omega_{ij})$ . In the back stress evolution equation  $f_1$  and  $f_3$  are material constants. In the drag stress evolution equation the value of  $m$  controls the hardening rate,  $Z_1$  is the saturated value of  $Z$ , and  $\dot{W}^I$  is the inelastic work rate. The parameter  $g_2$  in the damage evolution equation is a material function and damage growth is assumed to be proportional to

the maximum principal tensile inelastic strain rate  $\dot{\epsilon}_{\max}^{IT}$ . Initially damage is assumed to be absent in the material before loading. In the back stress relaxation equation  $\Omega_s$  is the steady state value of the back stress,  $\Omega_{\text{sat}}$  is the maximum saturated value of the back stress observed in uniaxial tensile tests, the constant  $\sigma_0$  is introduced to nondimensionalize stress, and B and r are material constants to control the time dependence. The proposed model reduces to that of Ramaswamy for  $\dot{\omega} = \omega = 0$ .

In uniaxial loading Rene' 95 response displays tension-compression asymmetry as shown in Figure 5. At constant strain rate the compressive tests saturate at a higher magnitude of stress than do the tensile tests. The experimental fatigue response as given in Figure 9 for example shows that for the same level of stress the tensile strain is less than the compressive strain. It is also shown in [5] that the minimum creep rates observed in compression are much less than those in tension at corresponding values of stress. These pieces of information are used to substantiate that a higher initial value of hardness for the material in compression than in tension. For the uniaxial exercise this asymmetry was included in the model by having two drag stress state variables,  $Z^+$  and  $Z^-$  similar to kinematic hardening components. The corresponding evolution equations are:

Tensile Drag Stress Evolution Equation,

$$\dot{Z}^+ = m^+(Z_1^+ - Z^+) \dot{W}^I \quad (7)$$

and

Compressive Drag Stress Evolution Equation,

$$\dot{Z}^- = m^-(Z_1^- - Z^-) \dot{W}^I. \quad (8)$$

When the stress is greater than zero  $Z=Z^+$  and when the stress is less than zero  $Z=Z^-$ . The  $\dot{Z}^+$  evolution equation was only active for stresses greater than zero and the  $\dot{Z}^-$  equation was only active for stresses less than zero.

#### IV. Evaluation of Material Parameters

The values of  $D_0$ ,  $n$ ,  $\Omega_{\max}$ ,  $Z_1^+$  and  $Z_1^-$  were found using a nonlinear regression analysis of the inelastic strain rates corresponding to saturated stress levels observed in the tensile tests. The values of the material constants  $f_1$ ,  $f_3$ ,  $m^+$  and  $m^-$  were determined using an iterative computer program with the tensile, creep, and cyclic test data as inputs. The program iterated until it converged on stable values for these material constants. For Rene'95 at 1200°F the values of  $Z_1^+$  and  $Z_1^-$  are equal.

The damage function,  $g_2$ , was determined as the final step after all other constants had been found. The damage growth was evaluated from the tertiary creep response for small values of accumulated inelastic strain and the long term fatigue response corresponding to large values of accumulated inelastic strain. Using both the creep and cyclic tests the values of  $g_2$ , relating damage to the accumulated inelastic strain, were found as shown in Figure 3. This damage curve demonstrates that the greatest damage growth occurs early in the loading of the specimen and the rate of damage accumulation approaches a steady-state value rather rapidly.

The maximum value of the back stress is observed in the short time tensile tests when the stress saturates. During long time loading such as creep, the maximum value of the back stress has a lower value than that in the short time tests. This lower value was seen by Ramaswamy [4] for Rene' 80 at 1400°F and 1600°F. This reduced back stress value is also present in

Rene' 95 at 1200°F. Figure 4 shows how the maximum back stress  $\Omega_s$  decreases from the maximum value  $\Omega_{sat}$  as a function of the applied stress. Without test data to for substantiation a lower bound has been artificially imposed. The value of  $\sigma_0$  was arbitrarily chosen as 200 Ksi to nondimensionalize stress. Since the time required for a given creep test to reach a stable back stress can be observed, the values of B and r were determined by a linear regression of the back stress relaxation equation and the test data.

#### V. Comparisons of Experimental and Calculated Results

The strain rate control test data for Specimens 1-1 and 6-1 in Figure 6 show that the saturation stress for Rene' 95 is essentially strain rate independent. The model predictions show a small amount of strain rate dependence; however the predictions are reasonable for both the stress rate controlled and strain rate controlled tests.

The comparison of the observed and predicted creep response is shown in Figure 7. The creep stresses range from 146 Ksi to 175 Ksi. The experimental data is ordered except for the 146 Ksi test. The model predicts reasonably well the primary, secondary, and tertiary creep responses for all of the tests except the 146 Ksi test. The slight dip in the predicted creep response connecting the secondary and tertiary creep regions is a consequence of matching the constants in the back stress relaxation equation with the damage growth equation. However, once the back stress is stabilized the model predictions are parallel to the experimental creep responses.

A typical stress control cyclic test is shown in Figures 8 and 9. The predicted and experimental peak strains as a function of time are shown in Figure 9. The experimental tensile peak strain is observed to remain relatively constant while the compressive peak strain decreases with each

additional loop until a steady state response is reached. The observed error in the model prediction is due to a combination of factors. However since test 5-3, Ref. [5], is for a stress range of  $\pm 168$  Ksi the deformation is well into the plastic range. It can be seen from the tensile tests in Figure 6 that a small deviation in the peak stress produces a large variation in the predicted tensile peak strain. Since the trends are clearly correct the predicted tensile strain is considered acceptable. Figure 8 shows how the shape of the fatigue loop changes with increasing cycles. A displacement limit of 0.02 in/in was defined as failure since the model does not include a criteria for the transition from damage accumulation to crack growth. The model has been used to predict the fatigue life up to cracking for two stress control tests 5-3 and 3-6 of Ref. [5] at  $\pm 168$  Ksi and  $\pm 158$  Ksi, respectively. In these calculations the damage growth appears to be reasonably accurate. Additional fatigue calculations will be made in the future to further evaluate the model. Finally, future work to use the model to predict the material deformation to combined creep and cyclic loadings is planned.

## VI. References

1. Kachanov, L.M., "Time to Fracture Under Conditions of Creep," *Mekhanika i Mashinostr.* No. 8, [in Russian], pp. 26-31, 1958.
2. Bodner, S.R. and Partom, Y., "Constitutive Equations for Elastic-Viscoplastic Strain-Hardening Materials," *ASME Journal of Applied Mechanics*, Vol. 42, pp 385-389, 1975.
3. Bodner, S.R., Partom, I., and Partom, Y., "Uniaxial Cyclic Loading of Elastic-Viscoplastic Materials," *ASME Journal of Applied Mechanics*, Vol. 46, pp 805-810, 1979.



4. Ramaswamy, V.G., "A Constitutive Model for the Inelastic Multiaxial Response of Nickel Base Superalloy Rene' 80," Ph.D. Dissertation, University of Cincinnati, 1985.
5. Stouffer, D.C., Papernik, L. and Bernstein, H., "On the High Temperature Response of a Super Alloy; Part 1: The Mechanical Properties of Rene' 95," AFWAL-TR-80-4163, 1980.
6. Stouffer, D.C., "A Representation for the Mechanical Response of IN100 at Elevated Temperature," AFWAL-TR-81-4083, 1981.
7. Abuefoutouh, N.M., "A Thermodynamically Consistent Constitutive Model for Inelastic Flow of Materials," Ph.D Dissertation, University of Cincinnati, 1983.

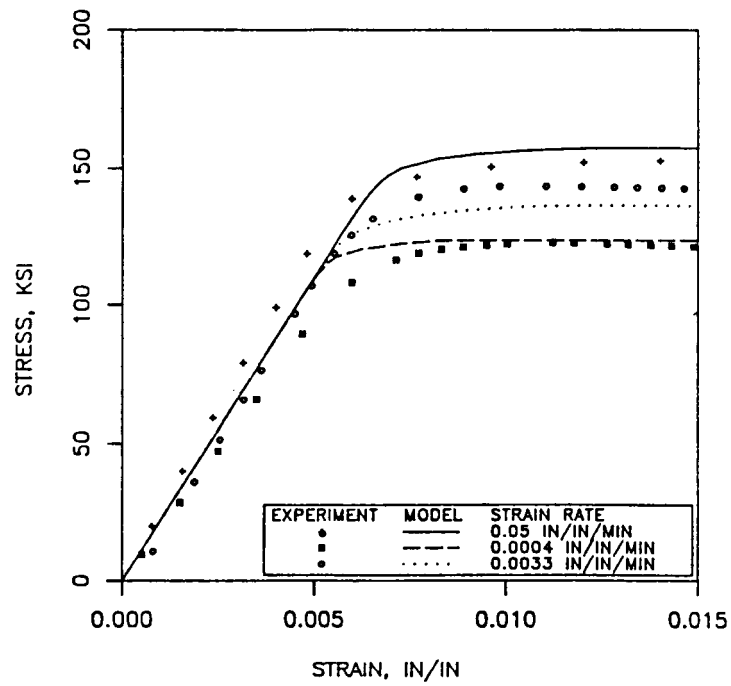


Figure 1. Predicted and Experimental Tensile Response of IN100 at 1350°F

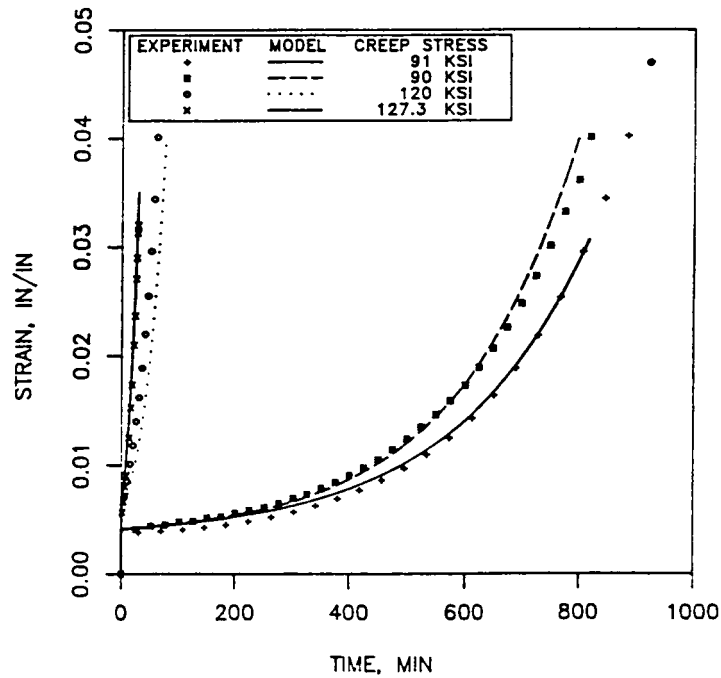


Figure 2. Predicted and Experimental Creep Response of IN100 at 1350°F

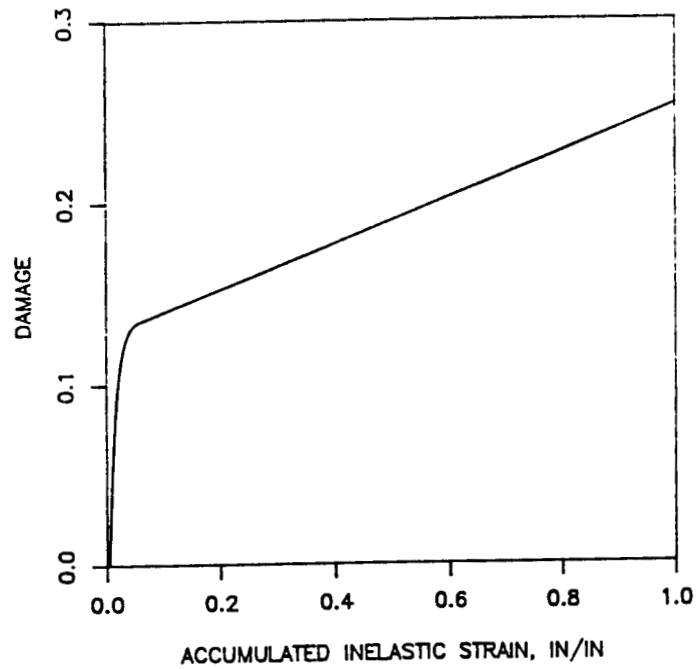


Figure 3. Damage as a Function of Accumulated Inelastic Tensile Strain for Rene' 95 at 1200°F

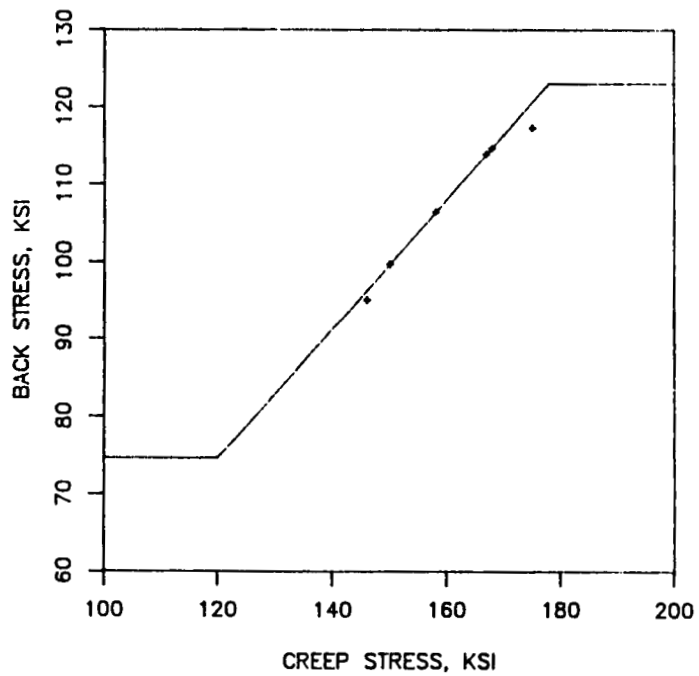


Figure 4. Variation of Saturated Back Stress with Applied Stress for Rene' 95 at 1200°F

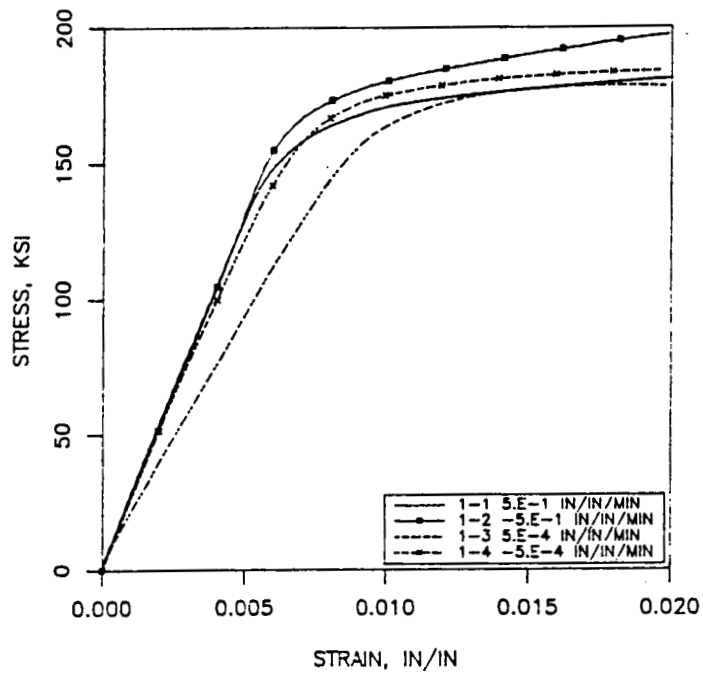


Figure 5. Comparison of Experimental Tensile and Compressive Responses of Rene' 95 at 1200°F

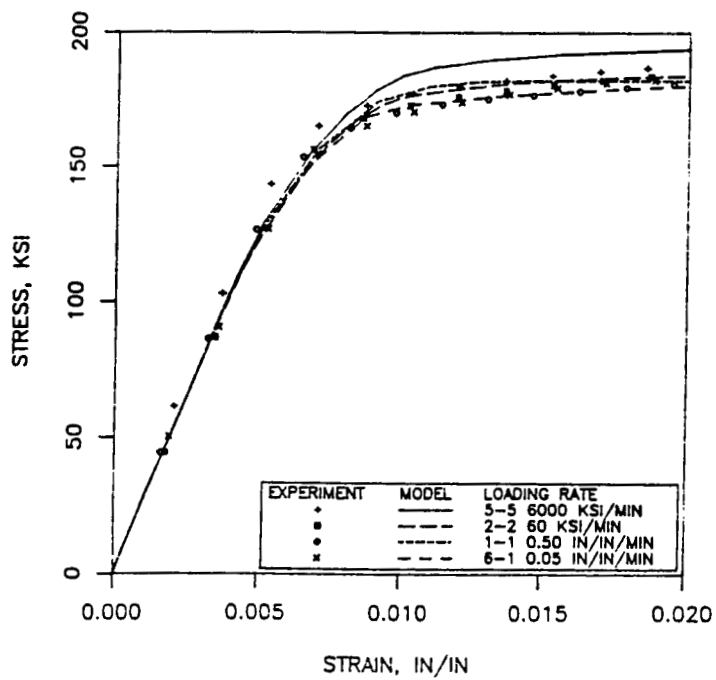


Figure 6. Predicted and Experimental Tensile Response of Rene' 95 at 1200°F

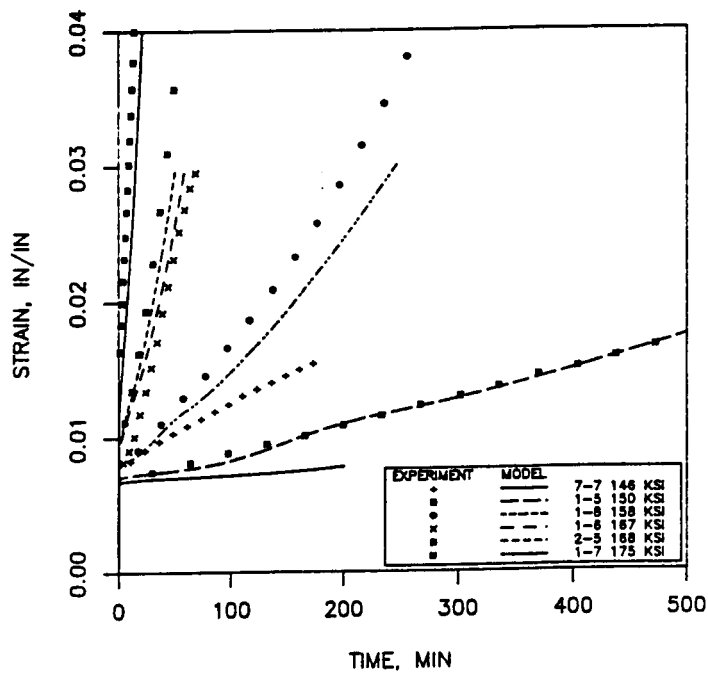


Figure 7. Predicted and Experimental Creep Response of Rene' 95 at 1200°F

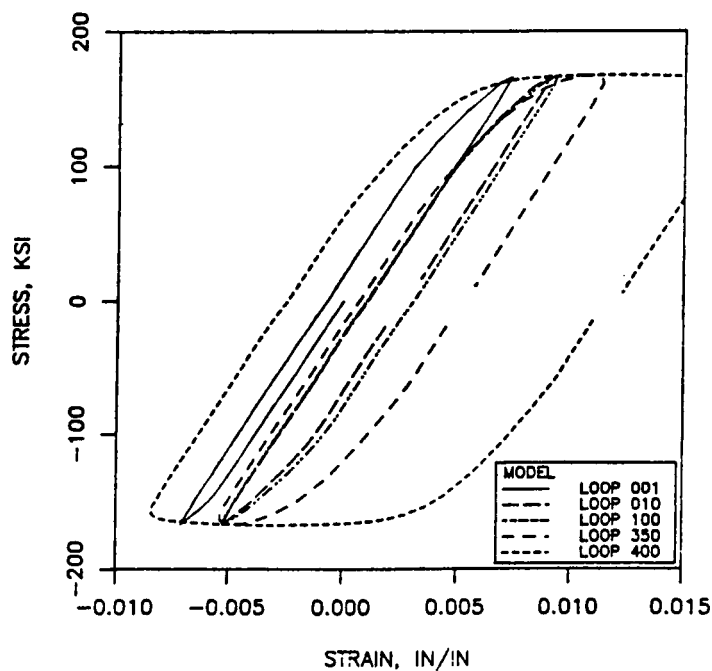


Figure 8. Variation of Fatigue Loop for Specimen No. 5-3 Loaded at  $\pm 168$  Ksi at 10 Cycles per Second for Rene' 95 at 1200°F

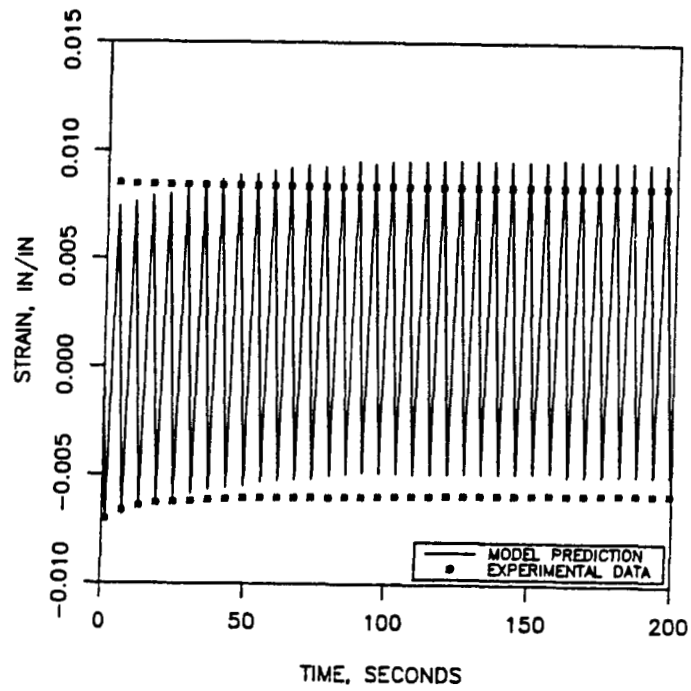


Figure 9. Predicted and Experimental Strains for Specimen No. 5-3 Loaded at  $\pm 168$  Ksi at 10 Cycles per Second for Rene' 95 at 1200°F